PHYSICAL REVIEW B **88**, 220405(R) (2013)

Multiple helimagnetic phases and topological Hall effect in epitaxial thin films of pristine and Co-doped $SrFeO_3$

S. Chakraverty,[1,*] T. Matsuda,[2] H. Wadati,[2] J. Okamoto,[3] Y. Yamasaki,[3] H. Nakao,[3] Y. Murakami,[3] S. Ishiwata,[2] M. Kawasaki,[1,2] Y. Taguchi,[1] Y. Tokura,[1,2] and H. Y. Hwang[1,4,5]

[1]*RIKEN Center for Emergent Matter Science (CEMS), Wako 351-0198, Japan*

[2]*Department of Applied Physics and Quantum Phase Electronics Center, University of Tokyo, Tokyo 113-8656, Japan*

[3]*Condensed Matter Research Center and Photon Factory, Institute of Materials Structure Science, High Energy Accelerator Research Organization, Tsukuba 305-0801, Japan*

[4]*Stanford Institute for Materials and Energy Sciences, SLAC National Accelerator Laboratory, Menlo Park, California 94025, USA*

[5]*Department of Applied Physics, Stanford University, Stanford, California 94305, USA*

(Received 12 September 2013; published 5 December 2013)

We report magnetotransport properties for epitaxial thin films of $SrFeO_3$ and $SrFe_{0.99}Co_{0.01}O_3$ with possible skyrmion-related spin textures. Resonant soft x-ray diffraction measurements revealed formation of helical spin structures for both samples ($Q//\langle 111\rangle$). From magnetotransport measurements we found several distinct helimagnetic phases with multiple/single Q vectors. A steep suppression of Hall resistivity is observed above the critical field to reach the high-field conical state, indicating the presence of skyrmionlike topological spin textures at lower fields responsible for the topological Hall effect.

DOI: 10.1103/PhysRevB.88.220405 PACS number(s): 72.25.Ba, 03.65.Vf, 12.39.Dc, 73.50.Jt

Topologically nontrivial spin textures have attracted considerable attention not only because of the rich physics related to the quantum Berry phase[1–9] but also because of their potential for novel spintronic functions.[10,11] One way to probe such unconventional spin structures is measurement of the Hall effect,[1–9] where conduction electrons acquire the Berry phase when following adiabatically the spin orientation of topological spin structures: the topological Hall effect (THE). One such topological spin texture is the skyrmion, which is made up of downward core spins, upward peripheral spins, and intervening swirling spins.[12–16] Such spin textures are observed in helimagnets containing several equivalent helical wave vectors (Q) to form a multi-Q structure. The formation of a skyrmionic crystal has been seen in reciprocal space by small angle neutron scattering[12] and in real space by using Lorentz transmission electron microscopy.[13]

So far, formation of skyrmionic crystals has been observed in chiral cubic (but noncentrosymmetric) B20-type compounds such as MX (M = Mn, Fe, Co; X = Si, Ge) and Cu_2OSeO_3,[11–16] beyond those arising from dipolar interactions in uniaxial ferromagnets.[17] Helimagnetic spin structures of these compounds are mediated by the Dzyaloshinskii-Moriya (D-M) interaction[18,19] in the noncentrosymmetry of their crystal lattice. Therefore, the spin swirling direction or the magnetic helicity is unique, depending on the chirality of the lattice as well as the sign of the spin-orbit interaction. On the other hand, the observation of skyrmion lattice formation has remained elusive in centrosymmetric compounds which have helimagnetic structure (with equal probability of right and left handed chirality) arising from other interactions, such as magnetic frustration, rather than the DM interaction.

Among many centrosymmetric perovskite oxides, it has been established that $SrFeO_3$ shows helimagnetic order.[20,21] Unlike B20-type compounds, the formation of spiral spin structure has been assigned to the competition between the ferromagnetic nearest-neighbor interaction and antiferromagnetic next-nearest-neighbor interaction,[20] or to the modified double-exchange mechanism with negative charge transfer energy.[22,23] Recently, Ishiwata *et al*. have demonstrated versatile helimagnetic (HM) phases and argued for the possible existence of multi-Q spin structures based on experiments using pulsed high (42 T) magnetic fields, in bulk single crystal of $SrFeO_3$.[24] However, the signature of topological Hall effect was not conclusive.[24] The major difficulty is that the critical magnetic field required to reach the single-Q conical state from a possible multi-Q state is rather high ($\sim$20 T) for this material, and this prevented the observation of the disappearance of the topological Hall effect in the high-field phase.

It is known that the HM structure of $SrFeO_3$ is easily transformed to the ferromagnetic (FM) state by partial substitution of Fe by Co.[25,26] A recent report has also demonstrated that a small amount (1%) of Co substitution can reduce the critical field ($\sim$10 T) between the two HM phases, which we infer are the multi-Q and single-Q conical spin structures, respectively,[27] as compared with the case of undoped $SrFeO_3$ ($\sim$20 T),[24] while keeping the global topology of the phase diagram very similar. For investigation of the topological Hall effect in this class of materials, growth of high-quality thin films are beneficial, because the transport properties can be precisely measured in a Hall device geometry. Despite intensive efforts in fabricating epitaxial $SrFeO_3$ thin films, however, the bulklike phase diagram has not been observed.[28,29] More specifically, the transition near 55 K in the resistivity was always absent. In this Rapid Communication, we report the fabrication of high-quality epitaxial $SrFeO_3$ (SFO) and $SrFe_{0.99}Co_{0.01}O_3$ [SFCO (1%)] thin films on $(LaAlO_3)_{0.3}(SrAl_{0.5}Ta_{0.5}O_3)_{0.7}$ (LSAT) (001) substrates, and demonstrate the emergence of nontrivial spin textures through the combination of transport and resonant soft x-ray diffraction (RSXD) measurements. RSXD has proved to be a powerful tool to study the magnetic structure of thin films, due to resonant enhancement of the $2p \rightarrow 3d$ absorption edge.[30–32] The RSXD (708 eV) experiments were carried out at beamline BL-16A in the Photon Factory, KEK, Japan.

We have used two steps to obtain fully oxidized SFO and SFCO (1%) thin films. At first, oxygen-vacancy-ordered brownmillerite-type $SrFeO_{2.5}$ and $SrFe_{0.99}Co_{0.01}O_{2.5}$ films were grown on atomically flat surface of LSAT (001) substrates by pulsed laser deposition. Then we oxidized these samples under ozone atmosphere at 200 °C for four hours, and cooled to room temperature under the same atmosphere. The out-of-plane θ–2θ x-ray diffraction (XRD) patterns show that the films (both ∼50 nm thick) are fully oxidized with (001) oriented perovskite structure. Figure 1(a) is the representative XRD pattern for the SFO film and LSAT substrate around the (002) Bragg reflection. Out-of-plane lattice parameter (c) is estimated from the (002) Bragg peak. Reciprocal space mapping around the (103) peak was performed to estimate in-plane lattice parameters [(a) and (b)]. Estimated lattice parameters are $a = b = 3.869$ Å and $c = 3.84$ Å, matching well with previous reports.[29] As shown in Fig. 1(b) [the (001) surface of the SFO film], an atomic step-and-terrace structure has been observed with no signature of cracking, ensuring high quality surface morphology of the film.

As shown in Figs. 1(c) and 1(d), the $Q = \langle qqq \rangle$ magnetic peaks emerge in both the compounds at low temperatures. The temperature dependence of the intensity and q value are also shown in Figs. 1(f) and 1(g). The magnetic Q vectors along the $\langle 111 \rangle$ direction as well as the q value in the SFO film are similar to that of bulk SFO, indicating that HM structures analogous to those in bulk are formed in the thin films. However, the temperature (∼105 K) where magnetic peaks appear for the SFO film is lower than that for bulk SFO (the highest-lying transition temperature $T_{N3} = 130$ K) and rather close to T_{N2} (the second transition temperature) for bulk SFO (=110 K).[24] Moreover, this temperature is slightly lower than that for the SFCO (1%) film. This Co-doping dependence of the transition temperature is rather similar to that for T_{N2} rather than T_{N3} in bulk SFCO.[27] These results therefore indicate that phase III, where the simple proper screw (single-Q HM) structure is formed in bulk samples, may be absent in thin films. That may have resulted from the lattice strain generated by the substrate or the reduced effective dimensionality of the electronic system in the thin film. The periodicities of the helical spin structures estimated from RSXD are 1.7 and 1.8 nm, for SFO and SFCO (1%), respectively; the periodicity becomes longer as Co concentration is increased in accordance with the case of bulk.[27]

Figure 1(e) shows the resistivity (ρ) of SFO, SFCO (1%) thin films and SFO bulk crystal (from Ref. 24) as a function of decreasing (solid line) as well as increasing (dotted line) temperature, in the absence of applied magnetic field (H_{app}). Two anomalies have been clearly observed for both thin film samples. Based on these anomalies, we constructed the zero-magnetic field magnetic phase diagrams of thin film samples of SFO and SFCO (1%), as shown with the color bars below the panel (e). For SFO film, the anomalies are observed at 46 K (T_{N1}) and 104 K (T_{N2}). In order to see the evolution of different HM phases with H_{app}, we performed extensive ρ measurements as a function of temperature at constant H_{app} (data not shown) and as a function of H_{app} at selected temperatures [Figs. 2(a) and 2(b)] for both samples. At least four phases for both SFO and SFCO (1%) samples could be unraveled through these extensive measurements, as

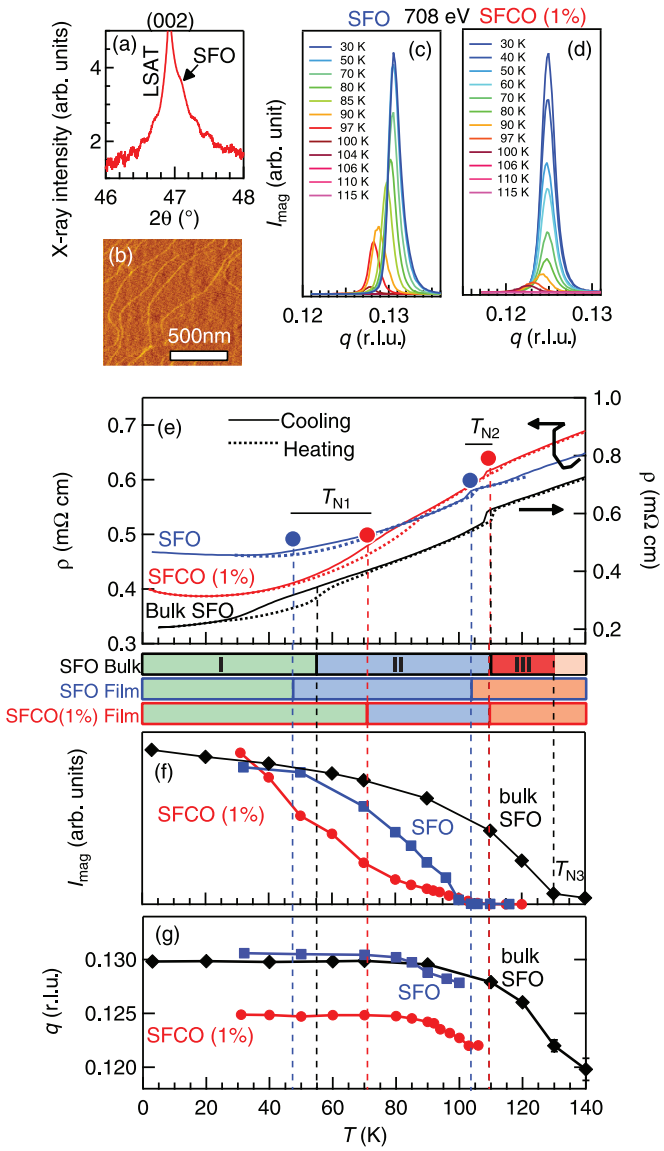

FIG. 1. (Color online) (a) θ–2θ x-ray diffraction pattern near the (002) Bragg reflection of $SrFeO_3$ film grown on LSAT (001) substrate. (b) AFM image of the (001) surface of the $SrFeO_3$ thin film. (c) and (d) $Q = (qqq)$ magnetic peaks for $SrFeO_3$ (SFO) and $SrFe_{0.99}Co_{0.01}O_3$ [SFCO (1%)], respectively, at various temperatures observed by RSXD measurements. (e) Resistivity (ρ) as a function of temperature in a decreasing (solid line) as well as an increasing (dotted line) temperature scan for SFO (blue) and SFCO (1%) (red) samples without applied magnetic field. The anomalies are marked with vertical broken lines. Resistivity data for bulk SFO in Ref. 24 are shown for comparison. The color bars below (e) represent the magnetic phase diagram [SFO bulk, SFO and SFCO (1%) thin films: top to bottom] in the absence of applied magnetic field. Temperature dependence of (f) intensity for the magnetic peaks and (g) the q value that were observed by RSXD. Neutron diffraction data for bulk SFO in Ref. 24 are shown for comparison.

plotted in Figs. 3(a) and 3(b). For convenience, we have used the same notation for each phase as used in previous reports.[24]

The ρ measurements at constant H_{app} have revealed that, as H_{app} is increased up to 14 T, T_{N1} and T_{N2} get closer to each other and almost merge, suggesting the presence (at $H_{app} < 14$ T)

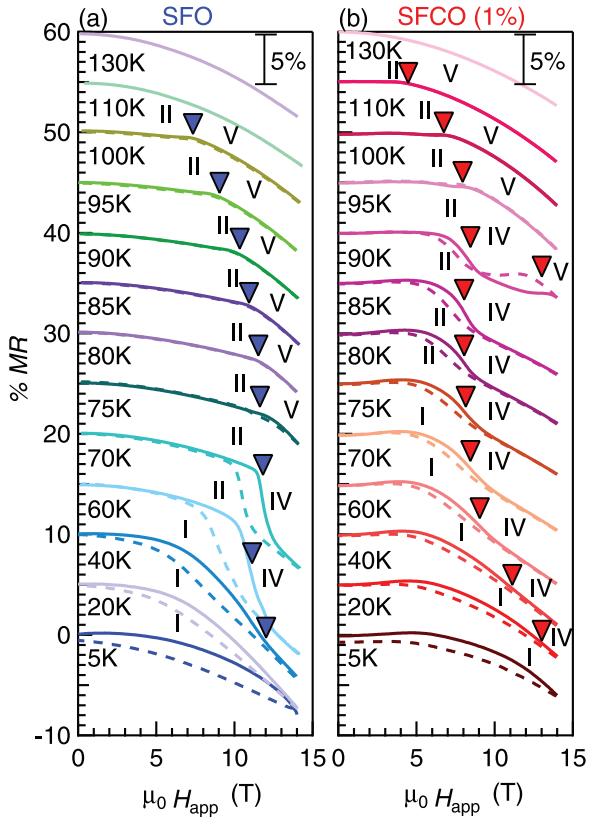

FIG. 2. (Color online) Magnetoresistance (MR $= [\rho(H_{app}) - \rho(H_{app} = 0)]/\rho(H_{app} = 0)$) as a function of applied magnetic field H_{app} at selected temperatures for (a) SFO and (b) SFCO (1%), respectively. Anomalies are marked with triangles. Solid lines represent increasing magnetic field scan and dashed lines represent decreasing field. Each data is shifted upward by 5% for clarity.

as well as the disappearance ($\geqslant$14 T) of the order phase (phase II) in between T_{N1} and T_{N2}. For the SFCO (1%) sample, T_{N1} and T_{N2} in the absence of H_{app} are 71 K and 110 K, respectively, and they merge at around 90 K under a much lower applied magnetic field ($H_{app} = 9$ T). After merging, this transition temperature decreases with further increase of H_{app}. We identify this transition as the boundary between phase IV and V, according to the notation defined in the high-field study of bulk SFO.[24] This suggests that phase II for SFCO (1%) exists within a much narrower region in the H_{app}-T plane in comparison with the SFO sample, and phase IV and V can be reached with a lower magnetic field (below 14 T) upon 1% doping of Co in SFO. In all the measurements performed under magnetic fields, the direction of H_{app} is out-of-plane along the [001] direction.

Phase I of the SFO thin film is characterized in terms of a large H_{app}-hysteresis and monotonic decrease of ρ with increase of H_{app}, as shown in Fig. 2(a). The magnetoresistance (MR) is defined by $[\rho(H_{app}) - \rho(H_{app} = 0)]/\rho(H_{app} = 0)$. At 40 and 60 K, anomalies have been observed at around 12 and 10.5 T, respectively. Such sharp transitions, with hysteresis, can be identified with the first order transition to phase IV (single-Q state).[24] It is important to note that the transition field to phase IV has been reduced for the SFO thin film as compare to bulk. The transition fields (marked with triangles)

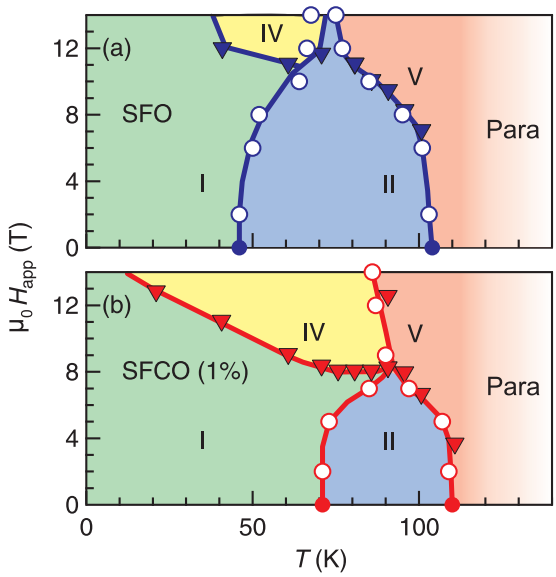

FIG. 3. (Color online) Magnetic phase diagrams of (a) $SrFeO_3$ (SFO) and (b) $SrFe_{0.99}Co_{0.01}O_3$ [SFCO (1%)] as constructed from ρ-T scans under various H_{app} (circles) and ρ-H_{app} scans at different temperatures (triangles also shown in Fig. 2).

are determined to be minima/maxima (phase I or II $\Rightarrow$ IV/II $\Rightarrow$ V) of $\frac{dMR}{dH_{app}}$. In phase I of the SFCO (1%) sample, an anomaly in the MR curve as well as hysteresis has also been observed, as shown in Fig. 2(b). This anomaly can be clearly identified as the first-order transition from phase I to IV. For both SFO and SFCO (1%), above T_{N2} (104 and 110 K, respectively) MR is quadratic with H_{app}. In phase II for both samples, by contrast, initially MR remains almost constant with increasing H_{app}, and then drops suddenly upon further increase of magnetic field. This implies that the helical spin structure in phase II as observed in RSXD may be different from a simple proper screw structure. Furthermore, for the SFCO (1%) sample at 90 K, reentrant behavior in MR accompanied with hysteresis was observed, corresponding to the successive first-order transitions II $\Rightarrow$ IV $\Rightarrow$ V (this feature was not observed in the SFO sample within the field range of the present experiment). This suggests that the nature of the spin textures in phases II, IV, and V are topologically different from each other.

To see the effect of spin textures on the transport properties further, the Hall resistivity (ρ_{yx}) was measured for both samples. Figures 4(c) and 4(d) show ρ_{yx} as a function of H_{app} at selected temperatures for SFO and SFCO (1%) samples. Based on these data, contour plots of ρ_{yx}/H_{app}, superimposed on the magnetic phase diagram, are shown in Figs. 4(a) and 4(b) (within the magnetic field range $H_{app} = 1$–14 T). Hall-resistivity measurements suggest that the thin film of SFO mimics the magnetic state of the bulk single crystalline sample [Figs. 4(a) and 4(c)].[24] Anomalously large values of ρ_{yx}/H_{app} have been observed in the low temperature region of phase I, which decreases with increasing temperature and again increases upon entering phase II. Finally, ρ_{yx}/H_{app} decreases and saturates to a lower value with further increase in temperature. On the verge of phase II and V, a clear signature of negative Hall resistivity has been observed, in accordance with the previous report on bulk SFO single crystal.[24] A slight

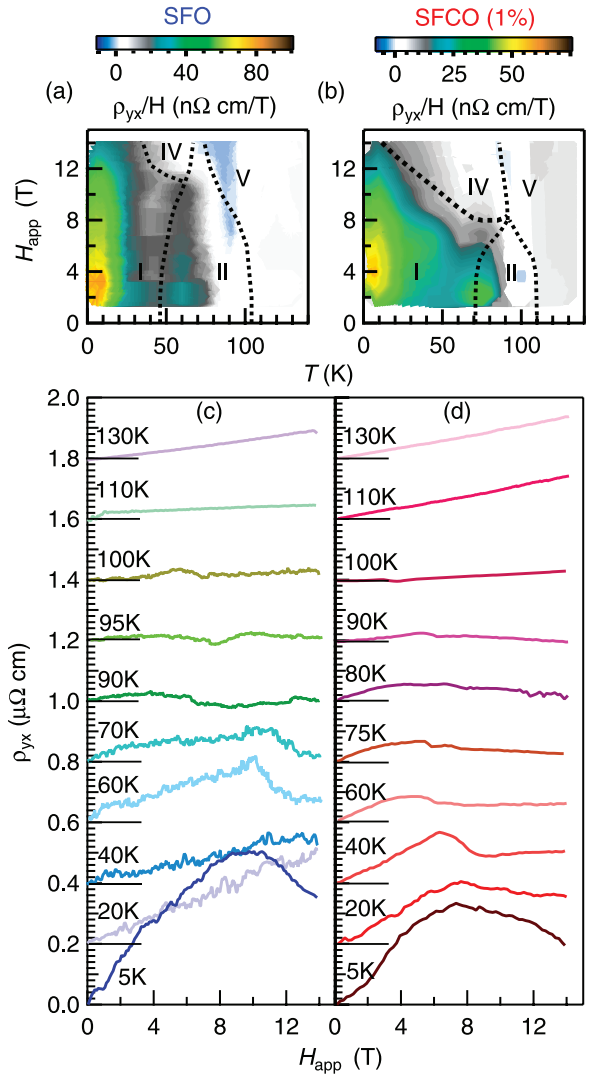

FIG. 4. (Color online) Contour maps of Hall resistivity ρ_{yx} divided by H_{app} (=1–14 T) for (a) SFO and (b) SFCO (1%), superimposed on the magnetic phase diagram. Magnetic field dependence of Hall resistivity at various temperatures for (c) SFO and (d) SFCO (1%), respectively. Each curve is shifted upward by 0.2 $\mu\Omega$ cm for clarity.

difference in quantitative features between present the thin films and the reported bulk single crystals might originate from the different measurement geometry ($H_{app} \parallel [001]$ for thin film and [111] for bulk) and lattice strain induced by the substrate.[24]

For SCFO (1%) [see Figs. 4(b) and 4(d)], a sharp decrease in ρ_{yx}/H_{app} has been observed with increasing H_{app} near the boundary between phase I and IV, especially at 40 K. Similar to the SFO sample, ρ_{yx}/H_{app} of SFCO (1%) at low H_{app} decreases with increasing temperature, and near the phase boundary between I and II it increases again. Thus, the value of ρ_{yx}/H_{app} (or Hall coefficient) is very sensitive to the species of the helimagnetic phase; it is very large as a metal in phases I and II (especially towards the lower temperatures within each phase) and sharply decreases upon undergoing the phase transitions of I $\Rightarrow$ IV and II $\Rightarrow$ IV.

These features are difficult to explain in terms of a conventional anomalous Hall effect (AHE) which is proportional to the magnetization, but is in accordance with the scenario of the topological Hall effect (THE) characteristic of the specific HM phases with spin chirality. In the THE, the conduction electrons coupled to the underlying spin texture can sense the fictitious magnetic field B^{z}_{eff}, or equivalently gain a Berry phase, when the spin texture is endowed with spin chirality or skyrmion number. The absence of spontaneous THE at $H_{app} = 0$ T [Figs. 4(c) and 4(d)], and its emergence (in phase I and II) in nonzero applied magnetic fields suggest that, in the absence of magnetic field, both hedgehoglike and antihedgehoglike textures form a periodic array, and that the imbalance between them (nonzero topological charge) is induced by a magnetic field, giving rise to THEs, as discussed in Ref. 9. From the present observations of the magnetic-phase dependent variation of the possible THEs [see Figs. 4(a) and 4(b)], phase I and II are assigned to forms of skyrmion crystals with multiple-Q vectors, while phase IV is a nontopological state, perhaps a single-Q conical phase.

In conclusion, we find multiple helimagnetic phases in $SrFeO_3$ and $SrFe_{0.99}Co_{0.01}O_3$ thin films. Resonant soft x-ray diffraction measurements confirmed the helical spin structures with propagation vector along the $\langle 111 \rangle$ direction. In contrast to bulk, the high-temperature proper screw phase seems to be absent in thin film form. By Hall measurements, several unconventional features, clearly distinct from an anomalous Hall effect of spin-orbit coupling origin, have been found uniquely in phases I and II, suggesting the formation of topologically nontrivial spin structures, such as three-dimensional skyrmion crystals composed of multiple $Q = \langle 111 \rangle$ helimagnetic states. This is a unique example of skyrmionlike spin structures arising from frustrated symmetric exchange interactions in a centrosymmetric crystal lattice.

This research is granted by the Japan Society for the Promotion of Science through the "Funding Program for World-Leading Innovative R & D on Science and Technology (FIRST Program)," initiated by Council for Science and Technology Policy (CSTP) and in part by JSPS Grant-in-Aid for Scientific Researh (S) Nos. 24224009, 24226002, and 21224008. H.Y.H. acknowledges support by the Department of Energy, Office of Basic Energy Sciences, Materials Sciences and Engineering Division, under contract DE-AC02-76SF00515. The synchrotron experiments were performed under the approval of the Program Advisory Committee (Proposal No. 2010G678) at the Institute of Materials Structure Science, KEK.

*suvankar.chakraverty@riken.jp

[1] J. Ye, Y. B. Kim, A. J. Millis, B. I. Shraiman, P. Majumder, and Z. Tešanović, Phys. Rev. Lett. **83**, 3737 (1999).

[2] Y. Taguchi, Y. Oohara, H. Yoshizawa, N. Nagaosa, and Y. Tokura, Science **291**, 5513 (2001).

[3] Y. Machida, S. Nakatsuji, Y. Maeno, T. Tayama, T. Sakakibara, and S. Onoda, Science **291**, 5513 (2001).

[4]P. Bruno, V. K. Dugaev, and M. Taillefumier, Phys. Rev. Lett. **93**, 096806 (2004).
[5]M. Onoda, G. Tatara, and N. Nagaosa, J. Phys. Soc. Jpn. **73**, 2624 (2004).
[6]A. Neubauer, C. Pfleiderer, B. Binz, A. Rosch, R. Ritz, P. G. Niklowitz, and Y. Böni, Phys. Rev. Lett. **102**, 186602 (2009).
[7]M. Lee, W. Kang, Y. Onose, Y. Tokura, and N. P. Ong, Phys. Rev. Lett. **102**, 186601 (2009).
[8]S. X. Hung and C. L. Chien, Phys. Rev. Lett. **108**, 267201 (2012).
[9]J.-H. Park and J. H. Han, Phys. Rev. B **83**, 184406 (2011).
[10]C. Day, Phys. Today **62**, 12 (2009).
[11]X. Z. Yu, N. Kanazawa, W. Z. Zhang, T. Nagai, T. Hara, K. Kimoto, Y. Matsui, Y. Onose, and Y. Tokura, Nat. Commun. **3**, 988 (2012).
[12]S. Mühlbauer, B. Binz, F. Jonietz, C. Pfleiderer, A. Rosch, A. Neubauer, R. Georgii, and P. Böni, Science **323**, 915 (2009).
[13]X. Z. Yu, Y. Onose, N. Kanazawa, J. H. Park, J. H. Han, Y. Matsui, N. Nagaosa, and Y. Tokura, Nature (London) **465**, 901 (2010).
[14]X. Z. Yu, N. Kanazawa, Y. Onose, K. Kimoto, W. Zhang, S. Ishiwata, Y. Matsui, and Y. Tokura, Nat. Mater. **10**, 106 (2011).
[15]A. Tonomura, X. Z. Yu, K. Yanagisawa, T. Matsuda, Y. Onose, N. Kanazawa, H. S. Park, and Y. Tokura, Nano Lett. **12**, 1673 (2012).
[16]S. Seki, X. Z. Yu, S. Ishiwata, and Y. Tokura, Science **336**, 198 (2012).
[17]X. Z. Yu, M Mostovoy, Y. Tokunaga, W. Zhang, K. Kimoto, Y. Matsui, Y. Kaneko, N. Nagaosa, and Y. Tokura, PNAS **109**, 8856 (2011).
[18]I. E. Dzyaloshinski, J. Phys. Chem. Solids **4**, 241 (1958).
[19]T. Moriya, Phys. Rev. **120**, 91 (1960).
[20]T. Takeda, Y. Yamaguchi, and H. Watanabe, J. Phys. Soc. Jpn. **33**, 967 (1972).
[21]H. Oda, Y. Yamaguchi, H. Takei, and H. Watanabe, J. Phys. Soc. Jpn. **42**, 101 (1977).
[22]M. Mostovoy, Phys. Rev. Lett. **94**, 137205 (2005).
[23]Z. Li, R. Laskowski, T. Litaka, and T. Tohyama, Phys. Rev. B **85**, 134419 (2012).
[24]S. Ishiwata, M. Tokunaga, Y. Kaneko, D. Okuyama, Y. Tokunga, S. Wakimoto, K. Kakurai, T. Arima, Y. Taguchi, and Y. Tokura, Phys. Rev. B **84**, 054427 (2011).
[25]S. Kawasaki, M. Takano, and Y. Takeda, J. Solid State Chem. **121**, 174 (1996).
[26]T. Takeda, S. Komura, and H. Fujii, J. Magn. Magn. Mater. **31**, 797 (1983).
[27]Y. W. Long, Y. Kaneko, S. Ishiwata, Y. Tokunaga, T. Matsuda, H. Wadati, Y. Tanaka, S. Shin, Y. Tokura, and Y. Taguchi, Phys. Rev. B **86**, 064436 (2012).
[28]N. Hayashi, T. Terashima, and M. Takano, J. Mater. Chem. **11**, 2235 (2001).
[29]H. Yamada, M. Kawasaki, and Y. Tokura, Appl. Phys. Lett. **80**, 622 (2002).
[30]H. Wadati, J. Okamoto, M. Garganourakis, Y. Scagnoli, U. Staub, Y. Yamasaki, H. Nakao, Y. Murakami, M. Mochizuki, M. Nakamura, M. Kawasaki, and Y. Tokura, Phys. Rev. Lett. **108**, 047203 (2012).
[31]S. Smadici, P. Abbamonte, A. Bhattacharaya, X. Zhai, B. Jiang, A. Rusydi, J. N. Eckstein, S. D. Bader, and J-M Zuo, Phys. Rev. Lett. **99**, 196404 (2007).
[32]S. Scagnoli, U. Staub, A. M. Mulders, M. Janousch, G. I. Meijer, G. Hammerl, J. M Tonnerre, and N. Stojic, Phys. Rev. B **73**, 100409(R) (2006).